A Step-by-Step Guide to Extracting Winding Resistance from an Impedance Measurement

Benedict X. Foo Aaron L.F. Stein Charles R. Sullivan
Thayer School of Engineering
Dartmouth College
Hanover, NH 03755 USA
Email: {Benedict.Foo.th, Aaron.L.Stein, Charles.R.Sullivan}@dartmouth.edu

***Abstract*—Impedance analyzer measurements can be helpful in assessing inductor and transformer winding resistance and predicting winding loss, but the measured ESR does not directly correspond to winding resistance. Neglecting the effects of core loss and winding capacitance can yield significant errors in the prediction. A step-by-step method to account for such effects and extract winding resistance from an impedance measurement is described. The proposed methodology is applicable to both inductors and multi-winding transformers. Several measurements are needed in this method; one is to determine the effects of core loss and the others yield the impedance from which winding resistance is extracted to form a resistance matrix. The winding resistance of a transformer was determined experimentally and the interactions between the winding resistance, effects of core loss, winding capacitance and inductance and their contributions to the measured impedance are demonstrated.**

I. Introduction

Magnetic component (i.e. transformer or inductor) design in power electronics remains an imposing challenge. Losses in a magnetic component can be attributed to both the windings and the magnetic material itself. Understanding how these losses vary with different operating conditions or different component designs is inherently difficult. There are a number of methods to measure core loss in the large-signal domain, some of which are described in [1]–[8]. The non-linearity of core loss leads to the need for such methods in order to predict the losses under relevant operating conditions.

Winding loss can be predicted by using a winding resistance matrix [9]. An impedance analyzer can be used to obtain the small-signal ESR of the component, but this measured result includes the effect of small-signal core loss as well as winding resistance. Capacitance also affects the result. Hence the need for a method to extract winding resistance from the measurement.

Having a clear way to extract winding resistance from an impedance measurement allows accurate prediction of winding loss. It also allows verification of the accuracy of winding loss models. Although extracting winding resistance might seem simple, there are a few common misunderstandings that can lead to significant errors in the predicted winding losses, as discussed in Section II. Although some of our previous work on winding loss has included extracting winding resistance from an impedance measurement [10], it was not explained in great detail. Hence, Section III will provide a step-by-step method to accurately extract winding resistance from an impedance measurement using just an impedance analyzer. Various measurement results will be presented in Section IV to show the importance of addressing the common misunderstandings as well as showing the effectiveness of the winding resistance extraction method.

A. Predicting Winding Loss with Winding Resistance

Before proceeding with the discussion of measurement and extraction methods, we briefly review calculations of winding loss from resistance. Winding loss in an inductor can be calculated by:

$$P_w = \sum_{n=0}^{\infty} R_w(nf_0) I_n^2 \tag{1}$$

where R_w is the winding resistance as a function of frequency, f_0 is the fundamental frequency, and I_n is the rms amplitude of the n^{th} Fourier series component of the winding current $i(t)$. For the case of a transformer, the winding loss can be written as

$$P_w = \sum_{n=0}^{\infty} \begin{bmatrix} I_{n,1} & I_{n,2} \end{bmatrix} \begin{bmatrix} R_{11}(nf_0) & R_{12}(nf_0) \\ R_{21}(nf_0) & R_{22}(nf_0) \end{bmatrix} \begin{bmatrix} I_{n,1}^* \\ I_{n,2}^* \end{bmatrix} \tag{2}$$

where $I_{n,1}$ and $I_{n,2}$ are the n^{th} Fourier series components of $i_1(t)$ and $i_2(t)$, respectively, in phasor form with RMS amplitude as the magnitude of the phasors, and $*$ indicates the complex conjugate. The winding loss effects are described by a frequency-dependent resistance matrix [9] in which R_{11} represents the resistance when only the primary winding is excited and R_{22} represents the resistance when only the secondary winding is excited. R_{12} and R_{21} represent the interactions between the windings. Capturing these interactions is important because the relative phase of the winding currents affects the winding loss significantly. For brevity, (2) was shown for only two windings; however, it can be extended to any number of windings.

From (1), one can predict winding loss of an inductor by determining the values of R_w, or from (2), one can predict winding loss of a transformer by determining the elements of the resistance matrix. This can be achieved by either using winding resistance models [11]–[14], or for greater accuracy, measuring the actual winding resistance using an impedance analyzer, which is the topic of this paper.

II. Common Mistakes with Winding Resistance Extraction

There are a few common mistakes made in using ESR measured with an impedance analyzer to predict power loss. Understanding the non-linearity of core loss is integral to understanding the basis of those mistakes.

Core loss is reflected in an impedance measurement as a contribution to the measured real part of impedance, also called effective series resistance or ESR. We consider two models to predict this contribution, R_c. At some excitation levels, they give significantly different values.

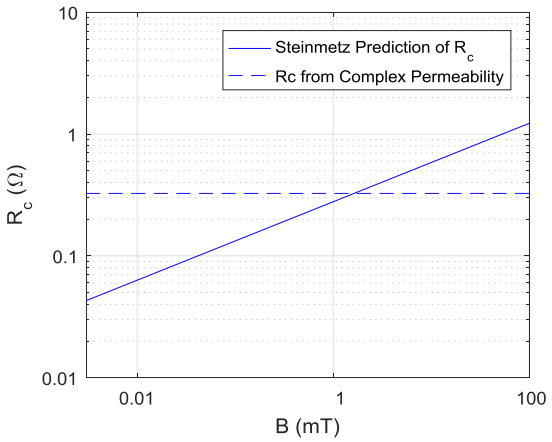

Fig. 1. R_c prediction using the Steinmetz equation and the complex permeability model of a 6-turn ungapped E-core (E30x15x7) of TDK N87 MnZn ferrite at 80 kHz.

Fig. 1 shows R_c of an inductor predicted separately by the two models; one based on complex permeability (dashed line), the other on the Steinmetz equation (solid line) [15], [16], both with parameters based on the data-sheet for TDK N87 ferrite. The complex permeability model results in an ESR reflecting core loss,

$$R_c = \mathrm{Re}\left(j\omega \frac{N^2}{\frac{\ell_e}{A_e \mu^* \mu_0} + \mathcal{R}_g} \right) \tag{3}$$

where N is the number of turns, $\mu^*\mu_0$ is the complex permeability of the material, A_e is the effective magnetic cross section, $\mathcal{R}_g$ is the gap reluctance, and ℓ_e is the effective magnetic path length inside the core.

The other model to predict R_c is derived from the Steinmetz equation in the appendix resulting in

$$R_c = 2 V_e k_1 \hat{I}^{\beta-2} \tag{4}$$

where V_e is the effective magnetic volume of the core material, β is a constant obtained from curve fitting of data provided by the manufacturer [15], [16] and k_1 is a constant at a particular excitation frequency

$$k_1 = k f^{\alpha} \left(\frac{N}{\frac{\ell_e}{\mu_r \mu_0} + \mathcal{R}_g A_e} \right)^{\beta} \tag{5}$$

Based on the Steinmetz model, one might argue that the core loss contribution can be neglected when interpreting the small signal measurements. As can be seen in Fig. 1, the Steinmetz model does predict very low values of R_c for small-signal excitation. However, the complex permeability is more accurate in this region, and results in much higher values of R_c, values that cannot be reduced by further reductions in excitation amplitude once the excitation is in the small-signal region. Based on Fig. 1, we hypothesize that R_c should be approximately constant over a range of small drive levels before starting to increase at higher drive levels. Section IV provides measurement data that confirm this hypothesis.

One common mistake is to equate the real part of the impedance measurement R_m to the winding resistance R_w, ignoring the effects of R_c. But as discussed above, R_c in the small-signal region cannot always be neglected. As confirmed in the experimental example in Section IV, the core loss and the winding capacitance both significantly increase R_m. Therefore, assuming $R_w = R_m$ and using that for (1) would overestimate winding loss.

Another common mistake is to assume that the impedance measured from a small-signal excitation captures the effects of both the winding and the core in a way that it could be used directly to calculate the total loss in the large-signal domain (i.e. $P_{total} = I_{rms}^2 R_m$). However from Fig. 1, R_c is actually higher in the large-signal domain than would be predicted by small-signal excitation. Hence the second mistake can lead to an underestimation of total loss.

A third common mistake is to measure the ESR of the winding without the core and equate that to winding resistance with the core. Measuring winding resistance without a core in order to eliminate core loss from R_m leads to an inaccurate estimate of R_w as the presence of the core affects the field shape in the region of the winding which changes the winding resistance by changing the proximity effect [11], [12]. This is true for both gapped and ungapped cores.

III. Methodology

A. Step-by-Step Guide to Winding Resistance Extraction

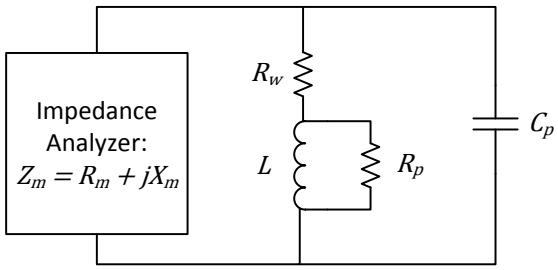

Fig. 2. Circuit model representing winding impedance for measurement interpretation.

Fig. 2 shows a model of an inductor connected to an impedance analyzer. The equivalent circuit includes the winding and core ESR (R_w and R_c) in series with the inductance L, and adds winding capacitance C_p in parallel. These components interact to produce R_m and we need to account for their effects in order to accurately extract R_w from the measured

impedance Z_m. L is extracted by measuring the impedance of the inductor at a low frequency ω, and then using $L = \frac{X_m}{\omega}$ where X_m is the imaginary part of Z_m as shown in Fig. 2. C_p is obtained by finding the inductor's self-resonant frequency ω_{res} and then using

$$C_p = \frac{1}{(\omega_{res})^2 L} \tag{6}$$

We can find the sum of the core and winding ESR values, R_{cw}, by correcting the real part of the measured impedance, R_m, for the effect of the parallel capacitance. The result is

$$\begin{aligned} R_{cw} = & \frac{1}{2C_p^2\omega^2 R_m} - \\ & \left(\frac{1}{2C_p^2\omega^2 R_m}\right)\left(\sqrt{2LR_mC_p^2\omega^3 - 2R_mC_p\omega + 1}\right) \\ & \left(\sqrt{-2LR_mC_p^2\omega^3 + 2R_mC_p\omega + 1}\right) \end{aligned} \tag{7}$$

where ω is the angular frequency at which the measurement is taken.

Obtaining R_c is non-trivial, as capturing R_c from an impedance measurement without the effects of R_w and C_p is challenging. To combat this, we recommend performing a separate measurement; a two-winding measurement similar to that described in [1], [17]–[19] to measure the small-signal core loss behavior. A transformer with the same core and number of turns in both the primary and secondary as the device under test, or DUT, but with no gap and much finer wire or fewer strands of litz wire is to be built for this measurement. If the DUT was an inductor, then the transformer to be built will have the same number of turns in the primary and secondary as the inductor. Fine wire keeps the proximity effect and winding capacitance in the windings low. A low proximity effect results in a low mutual resistance. A zero gap transformer results in a lower Q factor which makes the impedance measurements less difficult compared to a high Q factor. A diagram of the measurement set-up is shown in Fig. 3. The primary winding is excited by an ac current (through terminals Hc and Lc) and a voltage is measured across the secondary winding (terminals Hp and Lp). A summary of the terminals' functions is in [20], [21]. It is important that this measurement is performed in the small signal region (i.e. the core loss is independent of drive level).

Because the core measurement is performed with an ungapped core, the value of R_c measured here is different from that of the gapped transformer in Fig. 4. To find R_c of the gapped transformer, we first represent the core measurement result as a parallel RL combination. The value of the parallel core loss resistance, R_p, is independent of gap length. Please refer to the appendix for a detailed explanation of why this is true. Thus the value of R_p found with an ungapped core applies to the gapped transformer directly. To use this result in the model in Fig. 4, we transform the parallel RL combination to a series combination with

$$R_c = \frac{(\omega L)^2 R_p}{(\omega L)^2 + R_p^2} \tag{8}$$

The value of L used here is the inductance of the gapped inductor and not that of the ungapped core. We now have all the values we need to find R_w from (7) and (8) to get

$$R_w = R_{cw} - R_c \tag{9}$$

It is also possible to skip the measurement of R_p by using the complex permeability data provided by the manufacturer and (3) to obtain R_c if the correction is expected to be small. However this has a number of disadvantages. It might prove less convenient as the complex permeability varies with frequency and so multiple points are needed if the winding resistance is measured across a frequency range. Also, it might make the values of R_c used for (9) less accurate as the complex permeability measurement is performed on a different sample and it is unclear which excitation level it is performed at.

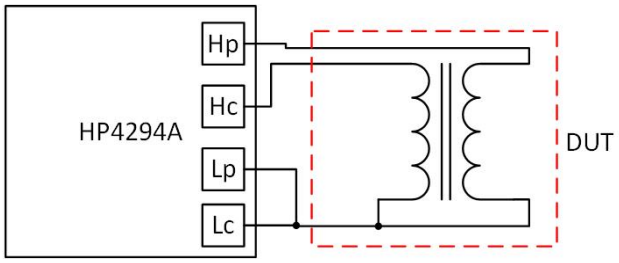

Fig. 3. Block diagram of small signal core resistance measurement.

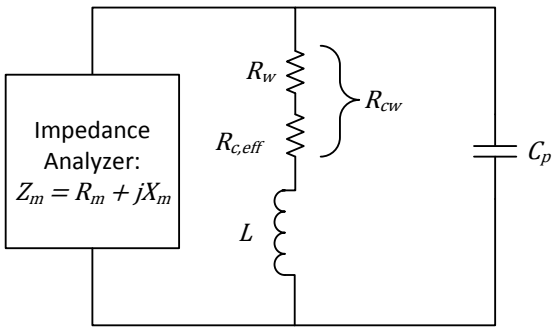

Fig. 4. Circuit model after R_p transformation.

B. From Impedance Measurement to Resistance Matrix

To obtain the resistance matrix shown in (2), we recommend performing three separate impedance measurements. Fig. 5 shows the three configurations recommended to obtain the resistance matrix: the first two measurements are of each winding driven individually, and the third is of both windings connected in a series opposing configuration such that only the leakage inductance is excited if the turns ratio is 1:1. R_{11} and R_{22} can be found by the first and second measurements, respectively, while the cross terms can be found from

$$R_{12} = R_{21} = \frac{(R_{11} + R_{22} - R_\ell)}{2} \tag{10}$$

where R_ℓ is obtained from the third measurement. In a 1:1 transformer, the series-opposing R_ℓ measurement does not require removing core loss effects because the magnetizing

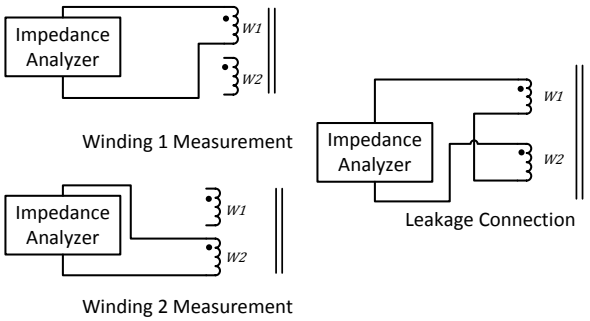

Fig. 5. Three winding connections to be measured for resistance matrix.

inductance is not excited. Note that (10) is most useful for low to moderate turns ratios and other measurements including short-circuit tests and series-aiding tests can also be used.

C. Practical Considerations

There are a few small but crucial practical considerations that we recommend in order to make precise impedance measurements. They include ensuring that no large metal objects are near the transformer when performing the measurement, and that the DUT is spaced above the table, ideally by using low-loss dielectric materials, to increase the separation between the DUT and any metallic object found in the table the DUT is measured on.

Picking a material that would lead to a low R_c would be useful if one were to use this winding extraction method to verify winding loss models. This is in order to keep R_c low compared to the winding resistance. The rule of thumb that we used was that R_c should be less than 10% of R_w across the frequency range of the measurement. A quick first-order method to choose a material for low R_c compared to R_w is to observe the complex permeability plot in the core material's data-sheet and use (3).

D. List of Steps of the Winding Resistance Extraction Method

Earlier in this section, the details of each step in the winding extraction method were given. For easy reference, the steps are summarized and listed in Table I.

TABLE I. STEPS TO THE WINDING RESISTANCE EXTRACTION METHOD

Step	Description
1	Measure impedance of DUT, $R_m + jX_m$
2	Compute $L = \frac{X_m}{\omega}$ using low-frequency X_m
3	Measure self-resonant frequency of DUT ω_{res}
4	Compute $C_p = \frac{1}{\omega_{res}^2 L}$
5	Measure R_p with a zero-gap transformer
6	Compute ESR of core and winding R_{cw} using (7)
7	Compute ESR of core R_c using (8)
8	Compute winding resistance $R_w = R_{cw} - R_c$

IV. MEASUREMENT RESULTS

A. Experimentally Verifying the Crossover Region Between Two Core Loss Models

Section II describes the non-linearity of core loss and the two models that predict R_c. The region in which one model transitions over to the other was experimentally verified by measuring the ESR of an ungapped inductor with an HP 4294A impedance analyzer. This inductor was designed to allow the impedance analyzer to drive the core into the nonlinear region. The frequency was chosen to be low enough that μ" was small so that even a small non-linear loss could be detected. An ungapped core was also used such that the drive level needed to go above that crossover point was reduced, allowing us to measure the crossover region using only an impedance analyzer. And finally, the number of turns for the winding was chosen such that there was an approximate impedance match with the HP 4294A's source resistance such that more energy gets coupled into the core.

Fig. 6 shows the measured behavior compared to the two models. Below a certain drive level, around 0.1 mT in this case, the measured ESR levels off at 225 $\mathrm{m}\Omega$ and does not continue to decrease as would be predicted by the Steinmetz model. The winding resistance of the same winding but without the core was measured at 80 kHz and found to be 27 $\mathrm{m}\Omega$ indicating that the measured ESR is dominated by R_c. Beyond 0.1 mT, however, R_c transitions into the non-linear loss region and begins to increase, following the Steinmetz model more closely.

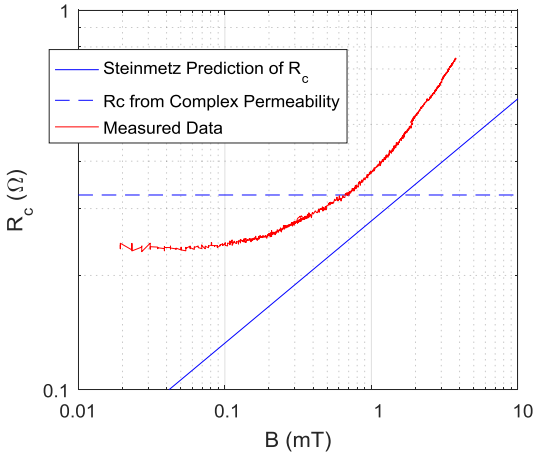

Fig. 6. The same R_c prediction plot in Section II shown together with actual measurement data. A 6-turn ungapped E-core (E30x15x7) of TDK N87 MnZn ferrite was built for this data with a litz wire constructed with 100 44 AWG strands for the winding.

There are a number of reasons for the discrepancy evident in Fig. 6 between the prediction and the measured data; it is unclear what drive level the measured complex permeability sweep was performed at, and the core shape was different from the core we used. This thus makes it important for an inductor designer to measure the actual R_c and not rely too heavily on the data provided by the manufacturer. Despite the discrepancy between data-sheet values and the measured values, the measurements confirm the hypothesis that there is a transition between Steinmetz behavior and linear behavior, and

that the ESR due to core loss does not decrease indefinitely as drive level is reduced.

B. Demonstrating the Need for a Winding Extraction Method

Two transformers with specifications shown in Table II were built to show the difference between the winding resistance and the measured resistance; they have the same windings, but had different core materials. The first set of measurements were performed on a transformer with TDK T38 material at frequencies well beyond the intended frequency range of the magnetic material to demonstrate the significance of R_c at higher frequencies. The transformer was measured with an HP 4294A impedance analyzer.

TABLE II. TRANSFORMERS USED FOR WINDING RESISTANCE EXTRACTION

Windings		
	Number of turns	28:28
	Number of layers in each winding	2
	Number of strands	100
	Strand gauge	44 AWG
Core		
Geometry	Pot core	30x19 Pot Core
Material 1	MnZn Ferrite	T38
Material 2	MnZn Ferrite	3F3
Gap	Centrepost and outer-ring	1.52 mm (3.04 mm total)

Fig. 7 shows the different resistances associated with the primary winding of the transformer. R_c becomes non-negligible as the frequency gets into the hundreds of kilohertz range. The actual winding resistance, R_w lies somewhere in between the measured resistance R_m and the winding resistance with an air-core, R_{air}.

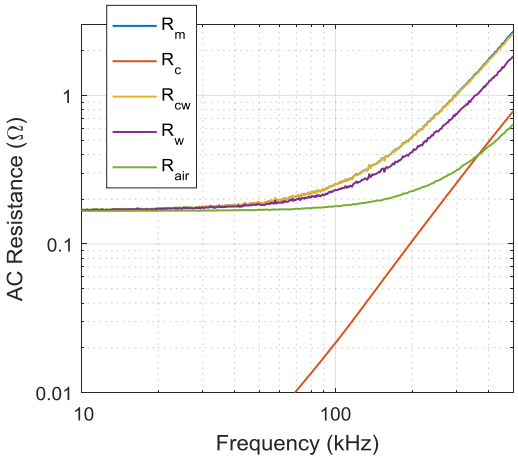

Fig. 7. How the different resistances vary with frequency as measured on the transformer with T38 as the core material with finer details listed in Table II. R_m is the real component of the measured impedance, R_c is the ESR that reflects core loss, R_{cw} is the series resistance after correcting for winding capacitance, R_w is the extracted winding resistance and R_{air} is the winding resistance of the same winding, but without the core.

Even with a low-loss core, correcting for core loss is important in winding resistance extraction. To show this, the TDK T38 core was replaced with Ferroxcube 3F3 of the same size and the same measurements were performed. Fig. 8 shows the resistance R_m normalized to R_w to highlight the importance of accounting for core loss and winding capacitance at the transformer's intended range of frequency (i.e. 3F3 material's intended operating frequency range). At frequencies close to 500 kHz, R_m overestimates R_w by over 20%. R_c approaches 20% of R_w at frequencies higher than 400 kHz indicating that it is not negligible even with a low-loss 3F3 core. This shows that correcting for winding capacitance and core loss is important. Fig. 8 also shows that measuring the resistance of the winding with the absence of the core will underestimate the winding resistance by over 10% at frequencies exceeding 350 kHz.

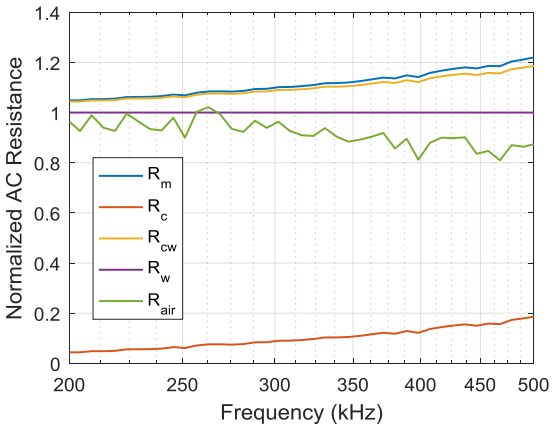

Fig. 8. Resistances normalized to R_w to show importance of extraction method. Measurements were performed on the transformer with 3F3 as the core material with finer details listed in Table II. Refer back to Fig. 7 for definitions of the different R values.

C. Showing that the Method Removes the Effects of Core Loss

To show that the method successfully removes the effects of the core, the resistance of the same pair of transformer windings used in the previous section was measured with the same two materials used for the core: a high loss material TDK T38 and Ferroxcube 3F3. If the winding loss extraction procedure works well, we expect to be able to extract the same resistance from both measurements, even though the measured resistance is very different.

Fig. 9 shows the measured resistance and extracted winding resistance of winding 1 of both transformers. Correcting for core loss for the 3F3 transformer results in only a slight correction since 3F3 has very low losses in this frequency range. The measured ESR of the T38 transformer deviates from $R_{w,3F3}$ by more than 20% as frequencies approach 100 kHz. After correcting for core loss however, the discrepancy at 100 kHz drops to under 10%. The remaining discrepancy could be explained by the two transformers having slightly different field shapes in the region of the windings. The initial relative permeability of the T38 core is 5 times greater than that of 3F3, and the 3F3 core has a hole in the center post whereas the T38 center post is solid, which would lead to a slightly higher winding resistance.

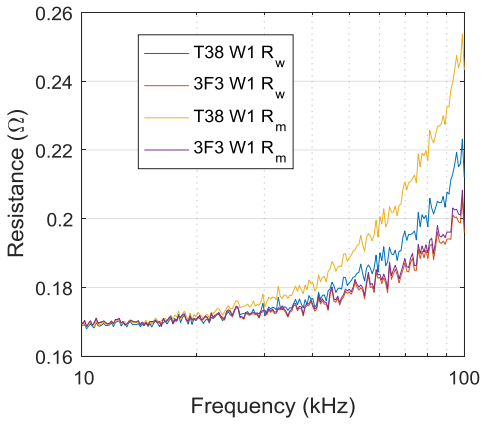

Fig. 9. Measured resistance and extracted winding resistance of two transformers with frequencies limited to 100 kHz.

D. Comparing Measured Data with a Winding Loss Model

The measured winding resistances for the three different winding configurations shown in Fig. 5 were compared with a winding resistance model [14]. This winding resistance model gets inaccurate at frequencies close to the winding's self-resonant frequency. The self-resonant frequencies of the different winding conditions of the transformer described in Table II were pushed to higher frequencies by decreasing the winding capacitance by adding a layer of insulation between each layer of winding. This was achieved with polypropylene tape between each layer of winding.

For these measurements, the lower limit of the frequency range was extended down to 10 kHz to show the measured DC resistance and the upper limit was set to 500 kHz to match the upper limit of the material's intended operating frequency. The circles represent the data obtained from the winding extraction method and the solid lines are that predicted by the model. It is evident from Fig. 10 that the data obtained from the winding extraction method closely match a winding loss model.

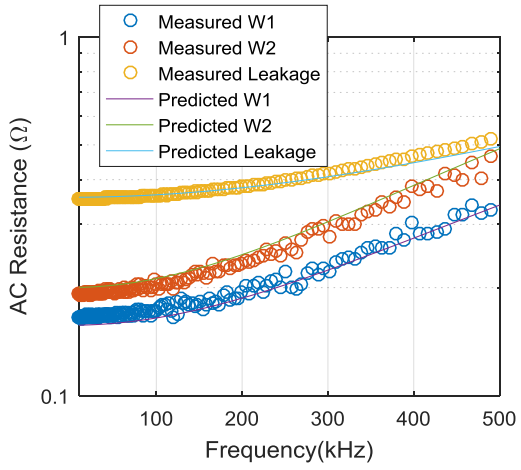

Fig. 10. Comparing the extracted winding resistance with that predicted by a winding loss model.

V. Conclusion

Knowing the winding resistance of an inductor or a transformer is imperative in magnetic component design. However, extracting the winding resistance from an impedance measurement involves a number of measurements and calculations. This paper provides a step-by-step guide on a winding extraction method that addresses the effects of the core and the winding capacitance.

Practical considerations were provided for precise impedance measurements, with an emphasis on core material choice for winding loss model verification. This paper also gives an explanation on how to use the impedance measurements to form a resistance matrix used to predict winding loss in magnetic components with multiple windings.

An inductor was built to demonstrate the non-linearity of core loss and the crossover region between two core loss models. The ESR that reflects core loss was shown to level off at low levels of excitation contrary to what the Steinmetz model predicts.

A transformer was built to present data on the extraction method and demonstrated that ignoring the effects of the core could lead to a 20% error, even with a low-loss material. It was also demonstrated that ignoring the effects of the core on the field shape in the region of the windings could lead to a 10% error.

The effectiveness of the method was also demonstrated by extracting the winding resistances of two transformers of the same winding but built with different core materials. Both winding resistances were found to be within 20% of each other. Lastly, the method was tested with a winding loss model and the extracted and predicted winding resistances matched each other very closely.

VI. Appendix

A. Derivation of R_c from the Steinmetz Equation

The derivation of (4) starts from the Steinmetz equation,

$$P_v = k f^{\alpha} \hat{B}^{\beta} \tag{11}$$

where k, α and β are constants [15], [16], f is the particular frequency of a sinusoidal excitation and $\hat{B}$ is the peak flux amplitude. In order to write (11) in terms of $\hat{I}$, a relationship between $\hat{B}$ and $\hat{I}$ is used

$$\hat{B} = \left(\frac{N\hat{I}}{\frac{\ell_e}{\mu_r \mu_0} + \mathcal{R}_g A_e} \right) \tag{12}$$

by substituting (12) into (11) we get

$$\begin{aligned} P_v &= k f^{\alpha} \left(\frac{N\hat{I}}{\frac{\ell_e}{\mu_r \mu_0} + \mathcal{R}_g A_e} \right)^{\beta} \\ &= k_1 \hat{I}^{\beta} \end{aligned} \tag{13}$$

which is algebraically equivalent to (11) where k_1 is a constant that absorbs all the relevant constants to make (13) concise

$$k_1 = k f^{\alpha} \left(\frac{N}{\frac{\ell_e}{\mu_r \mu_0} + \mathcal{R}_g A_e} \right)^{\beta} \tag{14}$$

Knowing that power loss is given by $P = RI_{rms}^2$, we can write the core loss as a function of R_c and $\hat{I}$

$$P_c = \frac{R_c \hat{I}^2}{2} \tag{15}$$

Since (13) is the power loss in the core per unit volume, we rewrite (13) as

$$P_c = V_e k_1 \hat{I}^{\beta} \tag{16}$$

where V_e is the effective magnetic volume. And finally from (16) and (15), R_c can be written as

$$R_c = 2V_e k_1 \hat{I}^{\beta-2} \tag{17}$$

B. Demonstration that R_p is Independent of Gap Length

If you excite a parallel impedance with an ac voltage source as shown in Fig. 11, the power loss in the circuit can be found by

$$P_{loss} = \frac{V^2}{R_p} \tag{18}$$

where V is the rms voltage of the driving source.

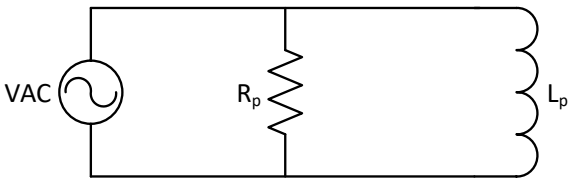

Fig. 11. Circuit model of a parallel impedance driven by an AC voltage source

The power loss in the circuit shown in Fig. 11 is thus only dependent on R_p. To explain how R_p is independent of gap length, we start from Faraday's law

$$\int v(t)dt = NA_eB \tag{19}$$

where $v(t)$ is the source voltage, and A_e is the effective magnetic area of the core. With the voltage constant, the flux density through the core, B, would also be constant and thus independent of the length of the gap. If B is constant, from (11), the power loss in the core is held constant. Finally from (18), if power loss is constant, R_p has to be independent of gap length as long as the drive level remains the same. It can also be shown from the reluctance model that the flux flowing in the core is independent of the reluctance as long as the transformer is driven by the same voltage.

ACKNOWLEDGMENTS

The authors thank Texas Instruments for partial support of this work.

REFERENCES

[1] A. F. Goldberg, "Development of magnetic components for 1-10 MHz dc/dc converters," Ph.D. dissertation, Massachusetts Institute of Technology, 1988.

[2] C. Xiao, G. Chen, and W. G. Odendaal, "Overview of power loss measurement techniques in power electronics systems," *IEEE Transactions on Industry Applications*, vol. 43, no. 3, pp. 657–664, 2007.

[3] D. Christen, U. Badstuebner, J. Biela, and J. W. Kolar, "Calorimetric power loss measurement for highly efficient converters," in *International Power Electronics Conference (IPEC)*. IEEE, 2010, pp. 1438–1445.

[4] J. M. Miller, C. W. Ayers, L. E. Seiber, and D. B. Smith, "Calorimeter evaluation of inverter grade metalized film capacitor ESR," in *Energy Conversion Congress and Exposition (ECCE)*. IEEE, 2012, pp. 2157–2163.

[5] D. Hou, M. Mu, F. Lee, and Q. Li, "New high frequency core loss measurement method with partial cancellation concept," *IEEE Transactions on Power Electronics*, 2016.

[6] Y. Han, G. Cheung, A. Li, C. R. Sullivan, and D. J. Perreault, "Evaluation of magnetic materials for very high frequency power applications," *IEEE Transactions on Power Electronics*, vol. 27, no. 1, pp. 425–435, Jan 2012.

[7] A. J. Hanson, J. A. Belk, S. Lim, C. R. Sullivan, and D. J. Perreault, "Measurements and performance factor comparisons of magnetic materials at high frequency," *IEEE Transactions on Power Electronics*, vol. 31, no. 11, pp. 7909–7925, 2016.

[8] V. J. Thottuvelil, T. G. Wilson, and H. A. Owen, "High-frequency measurement techniques for magnetic cores," *IEEE Transactions on Power Electronics*, vol. 5, no. 1, pp. 41–53, Jan 1990.

[9] J. H. Spreen, "Electrical terminal representation of conductor loss in transformers," *IEEE Transactions on Power Electronics*, vol. 5, no. 4, pp. 424–429, 1990.

[10] C. R. Sullivan, "Computationally efficient winding loss calculation with multiple windings, arbitrary waveforms, and two- or three-dimensional field geometry," *IEEE Transactions on Power Electronics*, vol. 16, no. 1, pp. 142–50, 2001.

[11] P. Dowell, "Effects of eddy currents in transformer windings," *Proceedings of the Institution of Electrical Engineers*, vol. 113, no. 8, pp. 1387–1394, 1966.

[12] J. A. Ferreira, "Improved analytical modeling of conductive losses in magnetic components," *IEEE Transactions on Power Electronics*, vol. 9, no. 1, pp. 127–131, 1994.

[13] A. M. Urling, V. A. Niemela, G. R. Skutt, and T. G. Wilson, "Characterizing high-frequency effects in transformer windings - a guide to several significant articles," in *Applied Power Electronics Conference and Exposition*. IEEE, 1989, pp. 373–385.

[14] D. R. Zimmanck and C. R. Sullivan, "Efficient calculation of winding-loss resistance matrices for magnetic components," in *Control and Modeling for Power Electronics (COMPEL)*. IEEE, 2010, pp. 1–5.

[15] E. Snelling, *Soft ferrites: properties and applications*. Butterworths, 1988.

[16] S. Mulder, "Power ferrite loss formulas for transformer design," *Power Conversion & Intelligent Motion*, vol. 21, no. 7, pp. 22–31, 1995.

[17] V. C. Valchev and A. Van den Bossche, *Inductors and transformers for power electronics*. CRC press, 2005.

[18] "Cores made of soft magnetic materials - measuring methods - part 1: Generic specification," *IEC 62044-1*, May 2002.

[19] "IEEE standard for test procedures for magnetic cores," *IEEE Std 393-1991*, pp. 1–64, March 1992.

[20] S. Prabhakaran and C. R. Sullivan, "Impedance-analyzer measurements of high-frequency power passives: techniques for high power and low impedance," in *Conference Record of the Industry Applications Conference*, vol. 2, Oct 2002, pp. 1360–1367.

[21] "New technologies for accurate impedance measurement (40 Hz to 110 MHz)," *Agilent Technologies*, 1999.